CD98hc (SLC3A2) participates in fibronectin matrix assembly by mediating integrin signaling

Chloé C. Féral,[1,2] Andries Zijlstra,[3,4] Eugene Tkachenko,[1] Gerald Prager,[1] Margaret L. Gardel,[5,6] Marina Slepak,[1] and Mark H. Ginsberg[1]

[1]Department of Medicine, University of California, San Diego, La Jolla, CA 92093
[2]Institut National de la Santé et de la Recherche Médicale, U634, Faculté de Médecine, 06107 Nice Cedex 2, France
[3]Department of Pathology, Vanderbilt University, Nashville, TN 37232
[4]Department of Cell Biology, The Scripps Research Institute, La Jolla, CA 92037
[5]Department of Physics and [6]Ben May Cancer Research Institute, University of Chicago, Chicago, IL 60637

Integrin-dependent assembly of the fibronectin (Fn) matrix plays a central role in vertebrate development. We identify CD98hc, a membrane protein, as an important component of the matrix assembly machinery both in vitro and in vivo. CD98hc was not required for biosynthesis of cellular Fn or the maintenance of the repertoire or affinity of cellular Fn binding integrins, which are important contributors to Fn assembly. Instead, CD98hc was involved in the cell's ability to exert force on the matrix and did so by dint of its capacity to interact with integrins to support downstream signals that lead to activation of RhoA small GTPase. Thus, we identify CD98hc as a membrane protein that enables matrix assembly and establish that it functions by interacting with integrins to support RhoA-driven contractility. CD98hc expression can vary widely; our data show that these variations in CD98hc expression can control the capacity of cells to assemble an Fn matrix, a process important in development, wound healing, and tumorigenesis.

Introduction

Fibronectin (Fn) is required for mammalian development and for blood vessel formation (George et al., 1993, 1997; Hynes, 1994; Peters and Hynes, 1996; Francis et al., 2002). Fn exists in both a soluble form in the plasma and as insoluble disulfide-bonded multimers in the extracellular matrix. The insoluble matrix form of Fn is essential for most of its biological functions in events such as wound healing, embryogenesis, and formation of the tumor microenvironment (Grinnell, 1984; Mosher, 1984; Ruoslahti, 1984). The soluble form of Fn is converted to the insoluble form by a process termed Fn matrix assembly, an active cellular process in which the soluble, dimeric Fn molecules are assembled into an insoluble, fibrillar pericellular matrix. Thus, an understanding of Fn matrix assembly is of broad biological significance.

Pioneering studies (McKeown-Longo and Mosher, 1983, 1985; Schwarzbauer, 1991; Sottile and Mosher, 1993; Sechler et al., 1996, 2001) have defined the regions of Fn important in the assembly process. The N-terminal 70-kD domain of Fn plays a pivotal role in matrix assembly. It does so by interacting with several other sites within the Fn molecule. These sites, which are generally contained within the type III repeats, are cryptic in soluble Fn and exposed as a consequence of conformational changes in Fn (Wierzbicka-Patynowski and Schwarzbauer, 2003). These conformational changes may involve extension of the Fn or unfolding of particular repeats. Studies from several laboratories show that Fn conformation can be changed by mechanical deformation (Zhong et al., 1998; Krammer et al., 1999; Erickson, 1994, 2002; Ohashi et al., 2002). Indeed, the hypothesis that matrix assembly site exposure is initiated by integrin-dependent mechanical deformation of Fn (Wu et al., 1995c) has been experimentally validated (Zhong et al., 1998). Thus, the assembly of an Fn matrix results from Fn–Fn interactions initiated by mechanical deformation of the Fn molecule.

The binding of Fn to integrins, such as $\alpha5\beta1$, initiates the matrix assembly process (Corbett and Schwarzbauer, 1999; Mao and Schwarzbauer, 2005). In particular, forces generated by the cytoskeleton and conveyed to Fn via integrins cause deformation of the Fn molecule (Zhong et al., 1998). For assembly to begin, these integrins must (1) physically associate

Correspondence to Mark H. Ginsberg: mhginsberg@ucsd.edu

Abbreviations used in this paper: DOC, deoxycholate; ES, embryonic stem; Fn, fibronectin; LPA, lysophosphatidic acid; MEF, mouse embryonic fibroblast; PECAM-1, platelet/endothelial cell adhesion molecule 1; WT, wild-type.

The online version of this article contains supplemental material.

The Journal of Cell Biology, Vol. 178, No. 4, August 13, 2007 701–711
http://www.jcb.org/cgi/doi/10.1083/jcb.200705090

with Fn, usually by binding it with high affinity (operationally defined as an "activated" integrin; Wu et al., 1995c), and (2) physically associate with the cytoskeleton (Wu et al., 1995c). Several signaling enzymes, including Src family kinases, pp125^{FAK}, Rho GTPases, and PI3 kinase, are also involved in the matrix assembly process (Wierzbicka-Patynowski and Schwarzbauer, 2002). These same signaling enzymes can be regulated by integrin ligation in a process referred to as outside-in integrin signaling (Boudreau and Jones, 1999; Arias-Salgado et al., 2005; Shattil, 2005). Thus, it is possible that integrin signals that regulate kinases such as pp125^{FAK} could participate in the assembly process.

We recently found that CD98hc, a type II transmembrane protein, mediates outside-in integrin signaling (Féral et al., 2005). CD98hc has two distinct functions: (1) it can associate with and regulate the function of selected integrins and (2) it can regulate the expression and distribution of CD98 light chains to modulate amino acid transport function. Each function depends on distinct domains within CD98hc, with the intracellular portion being required for interaction with integrins (Fenczik et al., 2001). Deletion of CD98hc in embryonic stem (ES) cells impaired the formation of teratocarcinomas in vivo and many integrin-dependent functions in vitro because CD98hc is a contributor to integrin-dependent biochemical signals (Féral et al., 2005). The role of CD98hc in integrin signaling suggested that it might participate in the Fn matrix assembly process. Here, we report that CD98hc is required for efficient Fn matrix assembly both in vitro and in vivo. Furthermore, deletion of CD98hc has little effect on Fn biosynthesis or integrin activation; instead, lack of CD98hc impairs outside-in integrin signals that result in RhoA-mediated cellular contractility necessary for Fn matrix assembly. Finally, the portion of CD98hc that interacts with integrins is necessary and sufficient to support cellular contractility and Fn matrix assembly. Thus, we find that CD98hc participates in Fn matrix assembly by mediating the outside-in integrin signals required for the contractile events that initiate and sustain Fn matrix assembly.

Results

CD98hc is involved in Fn assembly in vivo

To determine whether CD98 regulates matrix assembly in vivo, we examined the distribution of Fn in teratocarcinomas

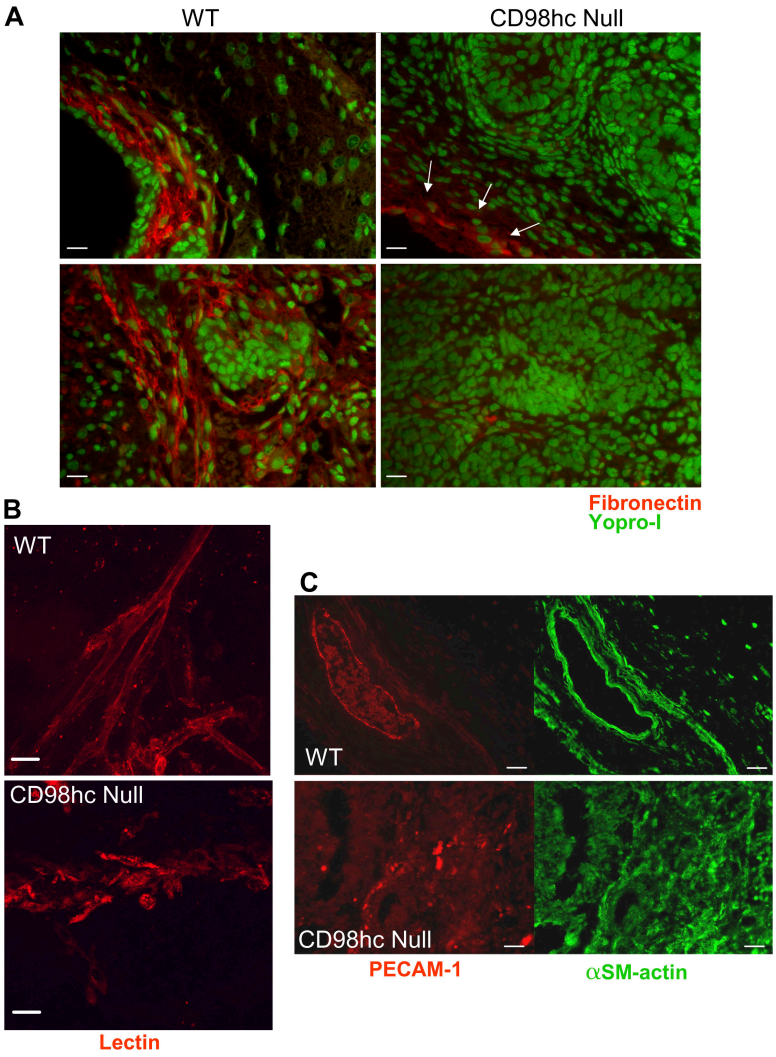

Figure 1. **CD98hc deficiency blocks Fn fibril assembly in vivo.** (A) Fn assembly was analyzed by staining WT (left) and CD98hc-null (right) tumors with an anti-Fn antibody. Fn staining is in red, whereas the nuclei are in green. Staining of two independent tumors per genotype is shown. Although CD98hc-null tumors do not show Fn assembly, Fn fibrils can be seen outside the tumor region (arrows). (B) Neovascularization during tumor development. Sections of tumors (WT and CD98hc null) were harvested and stained to reveal blood vessels. Whole mounts of tissue samples were stained with fluorescent IB4 lectin and analyzed by laser-scanning confocal microscopy. Sections (z series) were merged, and the resulting images are shown. (C) Immunofluorescent staining of WT and CD98hc-null tumors for the endothelial cells marker PECAM-1 (red) and smooth muscle cells marker α-smooth muscle (SM) actin (green). CD98hc-null tumors exhibit poor endothelial cell and smooth muscle cell organization. Bars: (A and C) 50 μm; (B) 200 μm.

formed in nude mice after subcutaneous injection of ES cells. As previously reported, injection of wild-type (WT) ES cells into nude mice led to the formation of large tumors. In contrast, CD98hc-null cells either did not form tumors or formed very small tumors (Féral et al., 2005). The CD98hc-null tumors that formed exhibited profound reduction in Fn fibrils, as judged by staining with a mAb against Fn (Fig. 1 A). In contrast, a prominent network of Fn was detected in the tumors formed by WT ES cells. Thus, CD98hc is involved in Fn matrix formation in vivo. Importantly, these CD98hc-null teratocarcinomas, like those formed from WT ES cells contain tissues from all three germ layers. Furthermore, absence of CD98hc is compatible with differentiation of multiple cellular lineages (Féral et al., 2005); hence, changes in cell lineages in the tumors are unlikely to account for the observed defect in matrix assembly. Thus, these results strongly suggest that lack of CD98hc resulted in a marked reduction in Fn matrix formation in vivo.

Because Fn is required for vascular development, we examined the blood vessels formed in the teratocarcinomas (Fig. 1 B) by whole-mount staining with endothelial cell–specific fluorescent-labeled lectin. We also visualized pericytes/smooth muscle cells and endothelial cells on these tumors by detection of the specific markers α-smooth muscle actin and platelet/endothelial cell adhesion molecule 1 (PECAM-1), respectively (Fig. 1 C). In the CD98hc-null tumors, endothelial cells were present but failed to form intact blood vessels (Fig. 1 B) or to invest with α-smooth muscle actin–expressing cells (Fig. 1 C). Instead of associating with endothelial cells, α-smooth muscle actin–expressing cells were dispersed throughout the tumors. In sharp contrast, WT tumors exhibited an organized network of blood vessels, including larger vessels with an endothelial lining and smooth muscle cell–containing intima and media (Fig. 1, B and C). Thus, the absence of CD98hc impairs Fn matrix deposition and vascular development, a process known to depend on Fn.

Lack of CD98hc impairs Fn matrix assembly in vitro

To learn whether CD98hc deficiency by itself leads directly to defective cellular Fn matrix formation and to understand the mechanisms by which CD98hc supports Fn matrix formation, we developed conditional CD98hc-null mouse embryonic fibroblasts (MEFs; Fig. 2, A and B). CD98hc conditional–null mice were generated as described in Materials and methods. We deleted CD98hc in vitro by infecting these cells with adenoviruses expressing Cre recombinase, resulting in 95% excision of exons 1 and 2 of CD98hc (Fig. 2 B). These cells were then mass sorted with immunomagnetic beads to select fibroblasts lacking detectable CD98hc (Fig. 2 C). Importantly, the CD98hc-null fibroblasts and parental WT cells expressed similar quantities of integrins α5, β1, α6, and αv, as judged by flow cytometry (Fig. 2 C) and showed defects in integrin signaling similar to those seen in CD98hc-null fibroblasts derived from ES cells (Fig. S1, available at http://www.jcb.org/cgi/content/full/jcb.200705090/DC1). None of the cells expressed

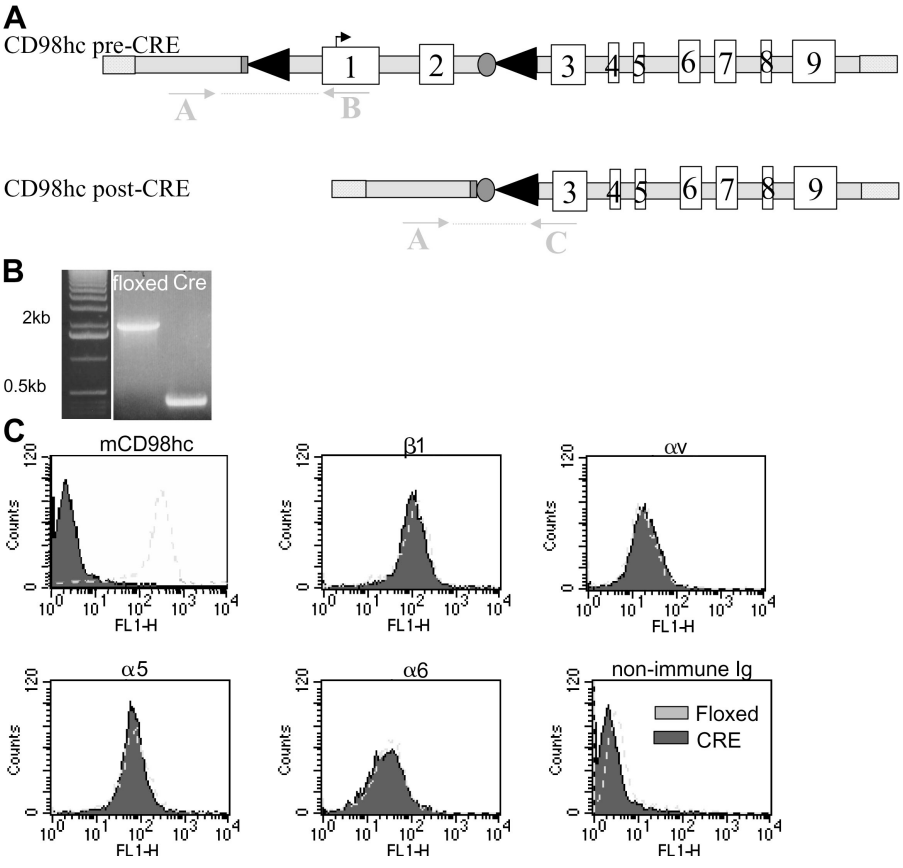

Figure 2. **Characterization of CD98hc-conditional allele.** (A) Conditional allele strategy. Representation of WT CD98hc locus and the targeted allele after CRE recombination (see Materials and methods). LoxP sites are depicted as triangles and Flp sites as ovals. (B) PCR analysis of genomic DNA after CRE recombination on MEFs. After the recombination occurred, CD98hc exons 1 and 2 were deleted. Expected sizes are 1.9 kb (floxed or WT allele; i.e., before CRE) and 382 bp (knockout allele; i.e., after CRE). (C) Flow cytometry analysis of cell surface expression of endogenous CD98 and of integrin subunits in CD98hc-deficient cells. WT cells are shown in dotted line and CRE cells in filled histogram. These FACS data show deletion of CD98hc in CRE cells (i.e., CD98hc null) and no change in integrin repertoire as a result of this deletion. Control is staining with irrelevant IgG.

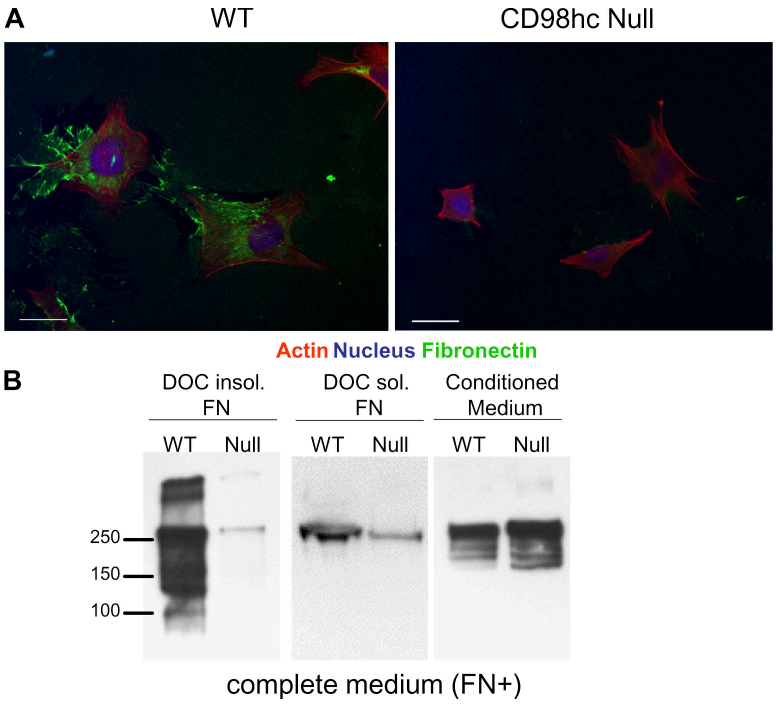

Figure 3. **Deletion of CD98hc blocks Fn assembly in vitro.** (A) WT (left) and CD98hc-deficient (right) MEFs were incubated for 48 h on 4 μg/ml Fn-coated coverslips. Fixed cells were stained for Fn (green) and actin (red). Nuclei appear blue. Note the absence of Fn fibrils in the CD98hc-null cells. Bars, 25 μm. (B) Fn assembly was also evaluated biochemically by analyzing the DOC-soluble and -insoluble portions of the cell matrix in both WT and CD98hc-null MEFs. Cells were cultured in complete medium (i.e., containing Fn). CD98hc-null MEFs were impaired in their ability to incorporate Fn in both their DOC-insoluble and -soluble pools in the presence of exogenous Fn. Level of Fn in the conditioned medium was similar for both WT and CD98hc-null cells.

a detectable amount of α1, α2, α4, or β3 integrins. Thus, these conditional CD98hc MEFs provide a tool to analyze the effect of CD98hc deletion on Fn matrix formation and integrin signaling by fibroblasts.

To examine Fn matrix assembly, we cultured WT or CD98hc-null fibroblasts and assessed matrix deposition by immunofluorescence. 48 h after plating, WT cells exhibited abundant Fn fibrils, whereas CD98hc-null cells (Fig. 3 A, green) were devoid of Fn fibrils (Fig. 3 A). Similar differences were observed regardless of whether the cells were subconfluent (Fig. 3 A) or confluent (not depicted). The lack of matrix was confirmed biochemically, by assaying the formation of deoxycholate (DOC)-insoluble Fn (Fig. 3 B), which was dramatically reduced in the confluent CD98hc-null fibroblasts. Because reduced assembly was observed in confluent CD98hc-null cells, the lack of matrix in these cells cannot be ascribed to reduced cell density (Wierzbicka-Patynowski and Schwarzbauer, 2003). Cell-associated Fn is present in fibroblast cultures in two separate pools, distinguishable on the basis of their solubility in DOC. One pool contains cell-bound DOC-soluble Fn, whereas the other one contains matrix-associated DOC-insoluble Fn. Fn matrix assembly proceeds by the binding of Fn to cells in the DOC-soluble pool with subsequent transfer and accumulation of assembled Fn in the DOC-insoluble pool (McKeown-Longo and Mosher, 1983). Although there was at least a 20-fold reduction in the DOC-insoluble Fn with the CD98hc-null cells (Fig. 3 B, left), there was only a modest, approximately twofold reduction in the DOC-soluble cell-bound Fn (Fig. 3 B, middle) and no decrease Fn in the conditioned medium (Fig. 3 B, right) compared with WT cells. Thus, CD98hc deletion leads to defective Fn matrix assembly, and the defect appears to be at the step of transfer from the DOC-soluble to -insoluble pool.

CD98hc-null cells' lack of Fn matrix is not due to reduced Fn biosynthesis or integrin affinity

Because CD98hc participates in amino acid transport (Deves and Boyd, 2000), we considered the possibility that CD98hc deficiency reduced the biosynthesis of Fn. To assess the availability of endogenous soluble Fn, we cultured the cells in medium containing Fn-depleted FBS (Fig. 4 A). Roughly twofold greater quantities of secreted soluble Fn were detected in the conditioned medium of CD98hc-null cells cultured in Fn-depleted medium (Fig. 4 A, left), and a profound reduction in DOC-insoluble Fn matrix was evident (Fig. 4 A, middle). This result suggests that both cell types produce similar quantities of Fn, but CD98hc-deficient cells cannot assemble the Fn, resulting in the increase in the conditioned medium. Furthermore, when we supplemented the cell cultures with an excess of plasma Fn, the CD98hc-null cells still failed to assemble a matrix (Fig. 4 B). Thus, CD98hc is required for Fn matrix assembly, but not for Fn synthesis or secretion, and the lack of assembly in CD98hc-null cells is not due to reduced Fn availability.

Matrix assembly requires that Fn first binds to high affinity (operationally defined as activated) integrins, such as α5β1, αIIbβ3, or αVβ3 (Wu et al., 1995a,b; Sechler et al., 1997, 2000). To assess the effect of CD98hc deletion on the affinity of Fn binding integrins in these MEFs, we examined their binding to a recombinant-soluble cell binding domain of Fn, composed of type 3 repeats 9–11 (3Fn[9–11]). The absence of CD98hc had no effect on the ability of the cells to bind to 3Fn(F9–11), a direct measure of the affinity of Fn binding integrins, such as integrin α5β1 (Chou et al., 2003). Importantly, when incubated with an activating anti–β1 integrin antibody, 9EG7, there was a marked increase in 3Fn(9–11) binding to both the WT and the null cells (Fig. 4 C); however, this enforced activation of

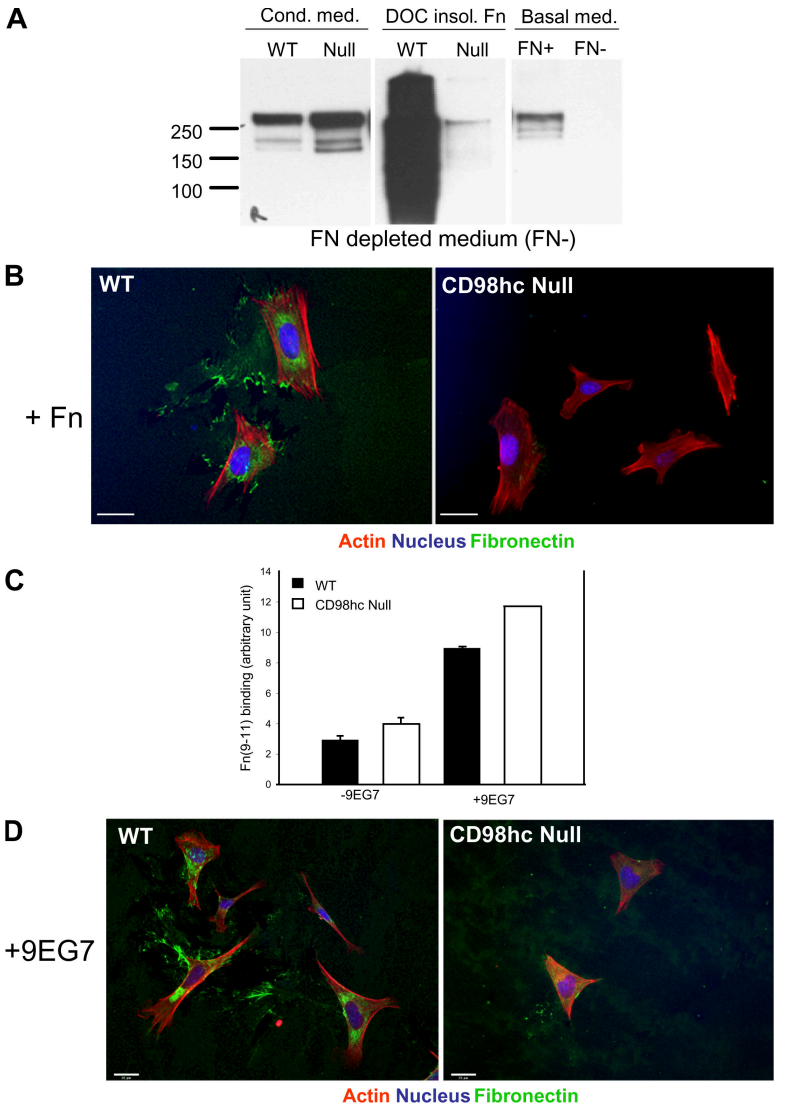

Figure 4. **CD98hc-null cells' loss of assembly is not due to deficient Fn biosynthesis or reduced integrin affinity.** (A) Fn biosynthesis was evaluated biochemically as described in Fig. 3. Levels of soluble Fn produced by WT and CD98hc-null cells (conditioned medium) were analyzed. Cells were cultured in Fn-depleted medium (Fn−). Both WT and CD98hc-null MEFs produced Fn, although only WT cells were able to assemble it into fibrils. Basal medium (Fn+) refers to complete Fn-containing medium. (B) WT (left) and CD98hc-deficient (right) MEFs were incubated for 48 h in the presence of 25 μg/ml exogenous soluble Fn. Fixed cells were stained for Fn (green), actin (red), and nucleus (blue). Addition of soluble Fn to CD98hc-null cell culture did not rescue Fn assembly. (C) Effect of activating anti-β1 mAb (9EG7) on α5β1 integrin binding to soluble Fn. Binding to the soluble cell binding domain of Fn (Fn 9–11) in the absence (−9EG7), and in the presence (+9EG7) of β1 activating antibody, are illustrated for WT (filled bars) and CD98hc-deficient (open bars) cells. Error bars indicate SEM. (D) WT (left) and CD98hc-deficient (right) MEFs were incubated for 48 h in the presence of 10 μg/ml activating β1 integrin mAb, 9EG7. Fixed cells were stained for Fn (green), actin (red), and nucleus (blue). Treatment of CD98hc-null cells with activating β1 mAb did not rescue Fn assembly in vitro. Note the presence of perinuclear intracellular staining for Fn in the CD98hc-null cells, consistent with Fn biosynthesis. Bars, 25 μm.

integrins did not rescue Fn assembly by the CD98hc-deficient cells (Fig. 4 D). Thus, the CD98hc-null cells' failure to assemble matrix is not due to a defect in their ability to synthesize or secrete Fn or to bind to soluble Fn with high affinity.

CD98hc mediates RhoA-driven traction forces on the extracellular matrix

Fn must be conformationally altered to initiate assembly into fibrils (Wierzbicka-Patynowski and Schwarzbauer, 2003). Once Fn binds to integrins, and the integrins connect to the cytoskeleton, RhoA-mediated cellular contractility exerts force on the Fn, leading to these conformational changes (Zhang et al., 1994; Zhong et al., 1998). We therefore examined the role of CD98hc in cellular contractility by assaying the contraction of an Fn-fibrin provisional matrix. Fibrin clots formed from blood plasma contain covalently cross-linked Fn that serves as a ligand for integrin α5β1–dependent matrix contraction (Corbett and Schwarzbauer, 1999). Incorporation of WT MEFs in these matrices led to a 52 ± 0.8% contraction after 2 h (Fig. 5, A and B). In contrast, contraction was markedly reduced when CD98hc-null cells were incorporated in the clot (24 ± 0.55% clot contraction). These cells lack β3 integrins, suggesting that the contraction was mediated by Fn binding β1 integrins, such as α5β1. Indeed, clot retraction was strongly inhibited by a function-blocking anti–mouse β1 antibody (clone Ha2/5; 18 ± 0.2 vs. 52 ± 0.8% clot contraction; unpublished data). Thus, CD98hc mediates the β1 integrin–dependent contraction of an Fn-fibrin matrix.

The finding that CD98hc was required for efficient clot contraction suggests that it mediates the generation of traction force on the extracellular matrix, a critical requirement for Fn assembly (Zhong et al., 1998). To examine this question, we used displacement of embedded fluorescent microbeads in flexible polyacrylamide substrates as a direct measure of traction forces (Beningo and Wang, 2002). Subconfluent MEFs were seeded for 2 h on Fn-coated polyacrylamide substrates in serum-free medium. Deformation of substrate caused by cellular traction forces was detected by tracing the displacement of fluorescent beads, and displacement vector maps, or strain maps, were generated (Fig. 5 C, green). The resulting strain maps demonstrated a marked reduction in traction forces exerted by CD98hc-deficient MEFs compared with WT cells (Fig. 5 C).

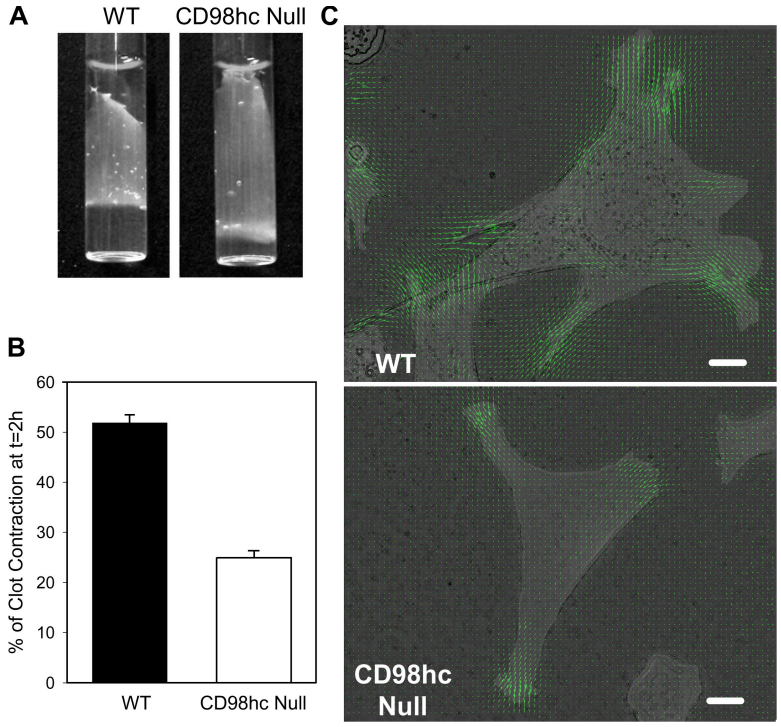

Figure 5. **CD98hc mediates cellular traction forces on the extracellular matrix.** (A) WT and CD98hc-deficient MEFs were mixed with 200 μl of Fn-containing platelet-poor plasma, 200 μl of 28 mM $CaCl_2$, and 5 U/ml human thrombin in Hepes-DME. Tubes were incubated for 2 h at 37°C. Depicted are digital images of WT and CD98hc-null clots. (B) Quantification of the percentage of clot contraction is presented (see Materials and methods). Values represent the mean ± SEM of triplicate determinations. The assay was repeated three times with similar results. (C) Decreased cellular traction forces in CD98-deficient MEFs. WT and CD98hc-deficient MEFs were plated on a 120-kD fragment of Fn-coated polyacrylamide sheets, in which fluorescent beads were embedded, as described in Materials and methods. Strain maps (green) overlaid with the brightfield images of WT (top) and CD98hc-null (bottom) cells plated on 120-kD Fn-coated polyacrylamide substrate (gray). CD98hc-deficient cells demonstrate reduced traction forces compared with WT cells. Bars, 10 μm.

There was about a threefold reduction in integrated strain for CD98hc-null cells compared with WT (0.77 vs. 2.5 pixels/area [arbitrary units], respectively; see Materials and methods). Thus, CD98hc-null cells are defective in the capacity to exert traction forces on the underlying substrate,

The small GTP binding protein RhoA is a major regulator of cell contractility (Chrzanowska-Wodnicka and Burridge, 1996; Hall, 1998) that provides the traction forces to initiate Fn matrix assembly (Zhong et al., 1998). Matrix assembly within tissues occurs when cells are in contact with surrounding 3D extracellular matrix, leading us to examine the effect of CD98hc deletion on adhesion-mediated alterations in RhoA activity when cells interact with 3D matrix (Cukierman et al., 2001). 30 min after adhesion of WT MEFs to a 3D matrix, RhoA activity decreased, followed by a secondary increase as previously described (Ren et al., 1999). In sharp contrast, the CD98hc-null cells did not show this late increase in RhoA activity (Fig. 6 A). Strikingly, both CD98hc-null and WT MEFs exhibited similar increases in RhoA activity in response to lysophosphatidic acid (LPA), an agonist that activates RhoA via G protein–coupled receptors (van Corven et al., 1989; Fig. 6 B). Thus, CD98hc is required for RhoA activation in response to cell adhesion to a 3D Fn matrix.

As noted, LPA induced RhoA activation in CD98hc-null MEFs, and activation of RhoA stimulates contractility, leading to the assembly of Fn by a variety of fibroblastic cells (Checovich and Mosher, 1993; Zhang et al., 1994; Kranenburg et al., 1997). Consistent with the capacity of LPA to induce RhoA activation in CD98hc-null MEFs, addition of LPA enabled CD98hc-deficient MEFs to contract a Fn-fibrin matrix (matrix contraction: WT, 32 ± 1.1%; CD98hc null, 10 ± 0.2%; LPA-treated CD98hc null, 52 ± 0.7%; Fig. 6 C). Similarly, LPA treatment enabled CD98hc-deficient cells to assemble an Fn matrix as assessed by quantifying formation of DOC-insoluble Fn (CD98hc null, 38 ± 6.3%; LPA-treated CD98hc null, 159 ± 3.3%, relative to WT MEFs; Fig. 6 D). Collectively, these data show that the reduced capacity of CD98hc-null cells to activate RhoA in response to extracellular matrix leads to their failure to assemble an Fn matrix.

The interaction of CD98hc with integrins mediates contraction of the extracellular matrix, thus regulating extracellular matrix assembly

The foregoing studies established that CD98hc participates in assembly of the Fn matrix by mediating adhesion-dependent RhoA activation that leads to traction on the extracellular matrix. Importantly, the CD98hc-null cells were able to activate RhoA in response to LPA, suggesting that matrix-driven RhoA activation is important in the assembly process. Integrins are the principal receptors that lead to matrix-initiated biochemical signals (Ingber, 1991; LaFlamme and Auer, 1996), and we previously found that the physical interaction of CD98hc with integrins is required for efficient integrin signaling (Féral et al., 2005). To examine the role of CD98hc–integrin interaction in matrix assembly, we reconstituted CD98hc-null MEFs with retroviruses encoding chimeras (Féral et al., 2005) formed between CD98hc and another type II transmembrane protein, CD69 (Fig. 7); each was well expressed as judged by flow cytometry (Fig. 7 B). The C98T98E69 (cytoplasmic domain CD98hc, transmembrane domain CD98hc, and extracellular domain CD69) chimera interacts with integrins, whereas C69T98E98 and C98T69E98 do not associate with integrins. Only the integrin binding chimera (C98T98E69) rescued the defect in Fn matrix assembly (Fig. 7 A) and contractility (Fig. 7 C). CD98hc-deficient cells expressing the chimera that binds to integrins (C98T98E69) were able to induce a clot contraction (56 ± 1%) even more efficiently than WT cells (37 ± 0.8%). Thus, the capacity of

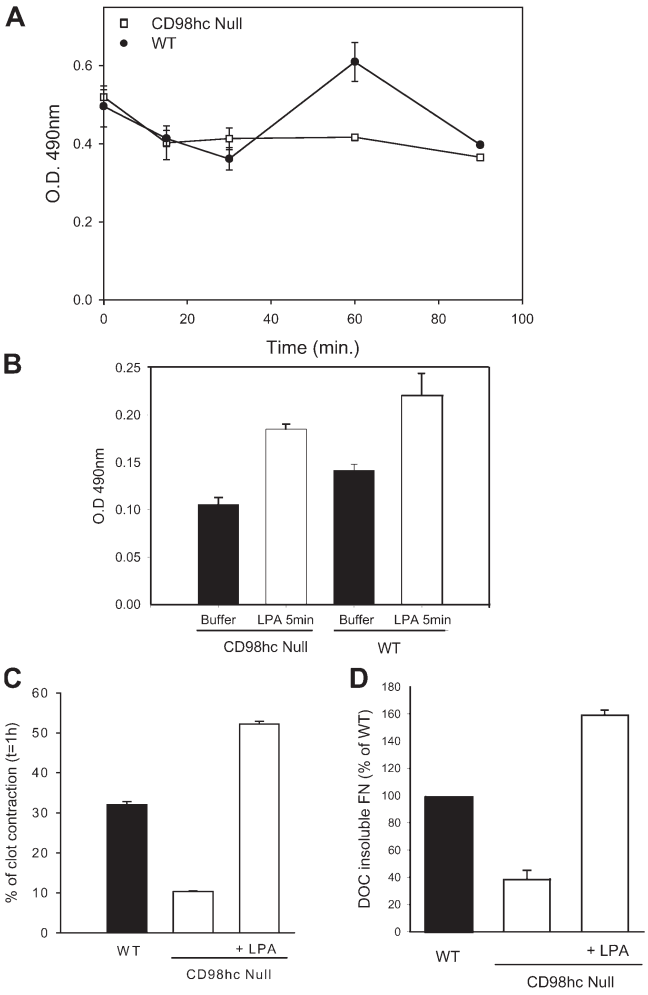

Figure 6. **CD98hc mediates adhesion-induced RhoA activation and matrix contraction to enable Fn matrix assembly.** (A) RhoA activity was measured in an ELISA-based Rho assay in WT and CD98hc-deficient cells after plating on a 3D Fn matrix. The error bars represent SEM. The assay was repeated three times with similar results. Samples were also resolved by SDS-PAGE and immunoblotted with anti-RhoA antibody (total RhoA) to confirm that both WT and CD98hc-null MEFs express similar amounts of total RhoA (not depicted). (B) Activation of RhoA by LPA in WT and CD98hc-null MEFs. Adherent serum-starved CD98hc-null cells were treated with 1 μg/ml LPA or buffer, and RhoA activity was measured after 5 min. Values represent the mean and range of duplicate determinations. The assay was repeated twice with similar results. (C) Activation of RhoA bypasses the defect in matrix contraction in CD98hc-null cells. Clot contraction was measured 1 h after WT, CD98hc-null, and CD98hc-null MEFs were stimulated with LPA (see Materials and methods for details). Values represent the mean ± SEM of triplicate determinations. Depicted is one of two such experiments with identical results. (D) Activation of RhoA bypasses the defect in Fn matrix assembly in CD98hc-null cells. DOC-insoluble Fn produced by WT, CD98hc-null, and CD98hc-null MEFs treated with LPA was evaluated biochemically as described in Fig. 3. CD98hc-null MEFs stimulated with LPA were able to assemble Fn into fibrils as efficiently as WT cells. Depicted are the means of triplicate measurements. The assay was repeated two times with similar results.

CD98hc to mediate contraction of an Fn-fibrin clot depends on its ability to interact with integrins.

Discussion

Fn matrix assembly can be conveniently divided into three steps. First, Fn binding integrins must be activated to bind Fn with high affinity (Wu et al., 1995c; Sechler et al., 1997). Recent studies (Tadokoro et al., 2003; Kuo et al., 2006) establish that integrin activation is mediated by talin binding to the integrin β cytoplasmic domain. Second, the integrins must connect to the actin cytoskeleton (Ali et al., 1977; Mautner and Hynes, 1977; Wu et al., 1995c), a connection that can be mediated by talin (Brown et al., 2002; Jiang et al., 2003). Third, cellular contractility exerts force on the integrin-bound Fn, deforming it and leading to the initiation of Fn matrix assembly (Zhang et al., 1994; Zhong et al., 1998). Here, we show that CD98hc participates in Fn matrix assembly and that it does so by physically associating with integrins to mediate matrix-driven activation of RhoA and the resulting cellular contractility that exerts force on the matrix.

The variable expression of CD98hc and its contribution to Fn assembly have implications for the relationship between cell proliferation and formation of the extracellular matrix. CD98hc expression is tightly regulated coordinately with cell proliferation (Diaz et al., 1997), a pivotal event in wound healing, tumorigenesis, and development. Repair of skin wounds depends on precisely controlled formation of a fibrous extracellular matrix. The extracellular matrix deposition correlates with proliferation of fibroblasts and endothelial cells within the damaged area (Midwood et al., 2004). The dramatic up-regulation of CD98hc in proliferating cells could thus serve to promote Fn matrix assembly in healing wounds; conversely, a failure to down-regulate CD98hc could lead to excess matrix deposition and cell proliferation, as seen in fibrosis and keloid scars (Muir, 1990). Similarly, the marked up-regulation of CD98hc in tumors (Deves and Boyd, 2000) could contribute to enhanced formation of Fn extracellular matrix, thus altering the microenvironment of cells during tumorigenesis (Weaver et al., 1996; Lelievre et al., 1998; Schmeichel et al., 1998; Bissell et al., 2002; Weaver and Gilbert, 2004). Moreover, we show that CD98hc mediates cell contractility, an event strongly associated with progression of some tumors (Paszek et al., 2005). Finally, the deposition of Fn along the blastocoele roof is reported to be a critical step in gastrulation (Boucaut et al., 1985) and later for morphogenetic movements driven by convergent extension (Davidson et al., 2006). This spatiotemporally regulated matrix assembly is controlled by the activity of cellular integrins, as manifested by their ability to promote cell spreading (Ramos and DeSimone, 1996; Ramos et al., 1996), a CD98hc-dependent process (Féral et al., 2005). Thus, the importance of Fn matrix assembly in development and the role of CD98hc in matrix assembly shown here provide a cogent explanation for the early embryonic lethality of CD98hc gene disruption (Tsumura et al., 2003) and suggest that changes in CD98hc expression, or its association with integrins, may influence a wide range of developmental processes through the regulation of Fn matrix assembly.

Materials and methods

Fn staining on tumor sections

A suspension of ES cells (1.5×10^6 cells per site) was injected subcutaneously into athymic BALB/c wehi nude mice. After 33 d, tumors were fixed in 10% formaldehyde, paraffin embedded, sectioned, and stained for Fn with a rabbit polyclonal antibody against human Fn (Sigma-Aldrich). Alexa Fluor 546

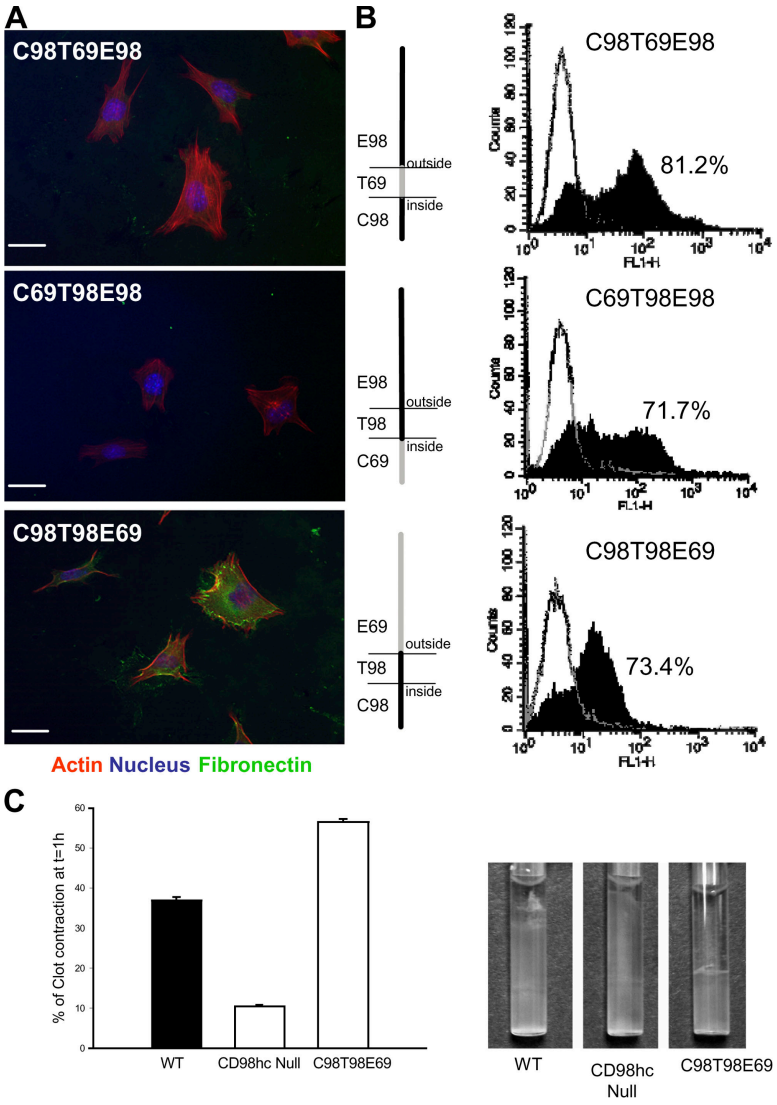

Figure 7. **CD98hc–integrin interaction mediates Fn assembly.** (A) CD98hc-deficient MEFs reconstituted with each chimera depicted in B (C98T69E98, C69T98E98, or C98T98E69) were treated as described in Fig. 3 A. Fixed cells were stained for Fn (green), actin (red), and nucleus (blue). Only C98T98E69 rescued CD98hc-deficient cells' ability to assemble Fn fibrils. Bars, 25 μm. (B) Expression and schematic of the chimeras used in A. CD98hc protein is depicted in black and CD69 in gray. Each chimera is defined by its cytoplasmic (C), transmembrane (T), or extracellular (E) domain derived from either CD98hc (98) or CD69 (69). CD98hc extracellular domain is necessary and sufficient for amino acid transport, whereas the intracellular and transmembrane domains are required for interactions with integrins (Fenczik et al., 2001). Flow cytometry analysis (right) of cell surface expression of exogenous chimeras in CD98hc-deficient cells (filled histogram) is shown. Control staining (empty histogram) was performed with irrelevant IgG. (C) CD98–integrin association is required for contraction of the extracellular matrix. WT, CD98hc-deficient, and CD98hc-deficient MEFs reconstituted with C98T98E69 were mixed with 200 μl of Fn-containing platelet-poor plasma, 200 μl of 28 mM $CaCl_2$, and 5 U/ml human thrombin in Hepes-DME. Tubes were incubated for 1 h at 37°C. Depicted are digital pictures of clots, as well as the calculated percentage of clot contraction (see Materials and methods). Values represent the mean ± SEM of triplicate determinations.

goat anti–rabbit IgG (H+L; Invitrogen) was used as a secondary antibody. Sections were counterstained with the nuclear dye YOPRO-1 (Invitrogen).

Whole-mount lectin staining

Tumor samples were fixed in 10% formaldehyde for 30 min at room temperature, washed in 1× PBS containing 0.1 g/liter $CaCl_2$, and cut into small (2 mm^3) tissue blocks. The tissue blocks were then incubated in the calcium-containing PBS in the dark for 48 h at 4°C in the presence of 10 μg/ml isolectin GS-IB4 Alexa Flour 568 conjugate (Invitrogen). After washing, the stained tissues were analyzed using a laser-scanning confocal microscope (1024 MRC; Bio-Rad Laboratories, Inc.). Z-serial images were merged using Lasersharp software (Bio-Rad Laboratories, Inc.) to obtain a 3D impression of the tumor samples.

Sequential immunohistofluorescence

4-μm tissue sections were deparaffinized and treated with methanol containing 0.3% H_2O_2 for 30 min at room temperature. Antigen retrieval and staining were performed using standard procedures. In brief, sections were first stained for α-smooth muscle actin using mouse anti–human α-smooth muscle actin antibody (clone 1A4; DakoCytomation) diluted at 1:50 in PBS containing 3% BSA and 0.01% Tween 20 for 60 min at room temperature. After washing, sections were incubated with secondary antibody goat anti–mouse Alexa 546 (Invitrogen) at 1:500 in PBS containing 0.01% Tween 20. Second, the TSA kit (PerkinElmer) was used for PECAM-1 staining using purified rat anti–mouse PECAM-1 mAb (BD Biosciences). The bound antibodies were detected using biotin-conjugated rabbit anti–rat (Vector Laboratories) in combination with Streptavidin-FITC antibody (Vector Laboratories). Sections stained as above but in the absence of the primary antibodies served as the negative controls.

Generation of CD98hc-conditional cells

A P1 mouse ES cell clone containing the *CD98hc* gene was isolated from a 129Sv/J mouse library by PCR screening (Genome Systems, Inc.). The targeting vector consisted of a 1.4-kb 5′ homologous region and a 4.9-kb 3′ homologous region. The region of exon 1, encoding the transmembrane domain of CD98hc, was flanked with loxP site. A neomycin selection cassette flanked by Flp sites (provided by H. Beggs and G. Martin, University of California, San Francisco, San Francisco, CA) was inserted in intron 2. The linearized targeting construct was electroporated into R1 ES cells. G418-resistant colonies were selected for 7 d. Two homologous ES cell recombinants were identified by PCR analysis (forward primer A, 5′-GATAGACGGGAGTATTCAGCGAGGC-3′; and reverse primer B, 5′-CTCATGGTGCCTGCAGAAACGG-3′) and confirmed by Southern blotting. PCR products were obtained at the expected size: 248 bp for WT allele and 304 bp for conditional knockout allele. These clones were karyotyped and subsequently injected into E3.5 C57BL/6 host blastocysts. The blastocysts were then transferred into pseudopregnant foster females. A total of seven chimeric males (distinguished by coat color) were obtained and bred to WT C57BL/6 females. Germ line offspring were genotyped by preparing DNA from tail biopsy for the presence of the targeted allele. Heterozygote males were identified by PCR analysis. Homozygote CD98hc-conditional knockout mice were bred onto human β-actin FLPe deleter strain (The Jackson Laboratory) to excise the neomycin selection cassette. Mice were housed in the University of California, San Diego, animal facility, and experiments

were approved by the University of California, San Diego, Institutional Animal Care and Use Committee.

Cell culture

MEFs were derived from CD98hc-conditional knockout homozygote embryos. MEFs were cultured in complete DME high glucose (Invitrogen), supplemented with 10% FBS (HyClone), 20 mM Hepes, pH 7.3 (Invitrogen), 0.1 mM nonessential amino acid (Invitrogen), 0.1 mM β-mercaptoethanol (Invitrogen), and 2 mM L-Glutamine (Invitrogen). The CD98hc-null MEFs were generated by infecting CD98hc-conditional knockout MEFs with adeno-CRE encoding CRE recombinase. Viral titers ranged from 0.6 to 1.2 × 10^{12} U/ml. CD98hc deletion was detected by PCR (forward primer A, see the previous section; and reverse primer C, 5′-CAGGGTTCTGTGTATGTGGGCGG-3′) and confirmed by flow cytometry. Cells were stimulated with 2 μg/ml (unless otherwise mentioned) LPA (1-oleoyl-2-hydroxy-sn-glycero-3 phosphate, monosodium salt) as described elsewhere (Zhong et al., 1998). In brief, MEFs were plated at 1 million per 10-cm Petri dish and treated every 4–5 h for 18 h (starting 24 h after plating). The reconstituted cells were generated by infecting CD98hc-null MEFs with pBabe-Puromycin retrovirus encoding or CD98hc/CD69 chimeras (Fenczik et al., 2001). Viruses were generated in EcoPack 293 cells (CLONTECH Laboratories, Inc.), and viral titers ranged from 0.9 to 1.7 ×10^6 U/ml. After puromycin selection, chimera expression was confirmed by flow cytometry.

Visualizing/imaging Fn assembly

MEFs were seeded in 1% FBS at 10,000 cells/well in 24-well plates onto 12-mm coverslips coated with 4 μg/ml Fn and blocked with 0.5% BSA. Where indicated, either 25 μg/ml of exogenous plasma Fn or 10 μg/ml of activating anti-β1 mAb, 9EG7, was added to the culture medium. After 48 h in culture, the cells were fixed with 2% PFA in PBS for 20 min and permeabilized for 10 min with 0.05% Triton X-100. Fixed cells were washed with PBS, and nonspecific sites were blocked with 3% BSA before the addition of primary antibody (rabbit anti-Fn [Sigma-Aldrich]; 1:2,000) for 2 h at 37°C. Specific binding was detected using goat anti–rabbit antibody conjugated with Alexa 488 (Invitrogen). The actin cytoskeleton was visualized by incubating with rhodamine-conjugated phalloidin while the nuclei were stained with DAPI (Invitrogen). Individual coverslips were mounted in aqueous mounting media with anti-fade (Gel Mount; Sigma-Aldrich). Digital images were captured at room temperature with a charge-coupled device camera (Orca ER; Hamamatsu) using a standard upright fluorescent microscope (Axioplan 2 [Carl Zeiss MicroImaging, Inc.; Plan-Neo Fluar 20× objective with 0.50 NA) controlled by the image capture and processing program Openlab (Improvision). Photoshop (Adobe) was used to increase the γ of images.

Biochemical assessment of Fn assembly

To assess the Fn assembly biochemically, the DOC-soluble and -insoluble portions of the cell matrix were analyzed as described previously (Zijlstra et al., 1999). In brief, MEFs were plated at 3 million cells per 10-cm Petri dish in complete medium (Fn+) or Fn-depleted medium (Fn−). Fn-depleted medium was generated by depleting Fn from the FBS using gelatin Sepharose before preparing the medium (Zijlstra et al., 1999). The cells were incubated for 48 h, at which time the conditioned medium was collected. The cell monolayer was washed with 3× PBS and lysed in 2 ml 3% DOC, 50 mM Tris, pH 8.8, and 0.1 mM EDTA, with protease inhibitors (complete, mini protease inhibitor tablets; Roche) for 15 min at 4°C. The lysate was subsequently passed through a 23-gauge needle five times and spun at 35,000 *g* for 20 min to remove the insoluble material. The soluble component was kept for further analysis. The insoluble pellet was washed once with DOC lysis buffer and spun again. The pellet was solubilized in 50 μl reducing Laemmli buffer (62.5 mM Tris-HC1, pH 6.8, 1.5% SDS, 9% glycerol, 50 mM dithiothreitol, and 0.005% bromophenol blue). Samples were separated by SDS-PAGE and analyzed by Western blotting using rabbit anti-Fn antibody (Sigma-Aldrich) followed by an HRP-conjugated goat anti–rabbit IgG (Jackson ImmunoResearch Laboratories), and bands were visualized by chemiluminescence (Pierce Chemical Co.). Intensities of bands were quantified by scanning densitometry using ImageJ software.

Flow cytometry

Anti–mouse α_1 (clone Ha 31/8), anti–mouse α_2 (clone HMα2), anti–mouse α_4 (PS/2), anti–mouse α_5 (clone HMα5-1), anti–mouse α_6 (clone GoH3), anti–mouse α_v (clone RMV-7), anti–mouse β_1 (clone 9EG7) integrin, and anti–mouse CD98 (clone H202-141) were purchased from BD Biosciences and used at the recommended concentrations. Goat FITC-conjugated anti–rat IgG and goat FITC-conjugated anti–hamster IgG were obtained from Biosource International and were used as secondary antibodies for α_4, α_6, α_v, and β_1; murine CD98; and α_1, α_2, and α_5 detection, respectively. Fn 9–11 binding was assayed by two-color flow cytometry as previously described (Hughes et al., 2002) in the presence or absence of 10 μg/ml of activating anti-β1 mAb 9EG7.

Fibrin clot retraction assay

This assay was performed by modification of a published method (Ylanne et al., 1993). In brief, WT or CD98hc-deficient MEFs were harvested with trypsin-EDTA (Invitrogen), quenched with complete medium, washed twice with PBS one time, and resuspended at 8.5 million cells per milliliter in serum-free DME (Invitrogen) buffered with 25 mM Hepes. 350 μl of this cell suspension was added to 7 × 45 mm siliconized glass cuvettes (Sienco, Inc.). Then, 200 μl of human platelet–poor plasma anticoagulated with ACD (85 mM sodium citrate, 65 mM citric acid, and 104 mM glucose) was added, followed by 200 μl Hepes-buffered DME containing 28 mM $CaCl_2$ and 5 U/ml human thrombin (Sigma-Aldrich). Cuvettes were incubated at 37°C with 5% CO_2. Images were acquired with a digital camera at 1 or 2 h, and subsequently the 2D area of the clot was measured using ImageJ software. The percentage of clot contraction was calculated according to the following equation: percentage of clot contraction (t = 1 h) = 100 ([area at t = 1 h/area at t = 0] × 100).

Cellular tension measurements

Polyacrylamide gels with embedded fluorescent beads on coverslips were prepared using previously described protocol (Wang and Pelham, 1998) with some modifications (see the supplemental text, available at http://www.jcb.org/cgi/content/full/jcb.200705090/DC1). Cell culturing, image acquisition, and strain map construction were performed as follows. WT and CD98-deficient MEFs were harvested with trypsin-EDTA (Invitrogen), quenched with complete medium, washed twice with 1× PBS, and resuspended at 0.1 million cells per milliliter in serum-free DME (Invitrogen) buffered with 25 mM Hepes. Cells were kept in suspension for 1 h at room temperature, and 20,000 cells were plated on a polyacrylamide sheet. After culturing on a polyacrylamide sheet for 2 h, images of both cell types were acquired within 10 min from each other. A microscope (TE2000; Nikon) equipped with environmentally controlled enclosure (37°C and 5% CO_2), 60× 1.2 NA water objective (Olympus), motorized stage (Ludl), excitation filter wheel (Ludl), filter set (Semrock), and camera (CoolSnap HQ; Roper Scientific) was used to acquire images of fluorescent beads embedded in polyacrylamide and brightfield images of cells in six different fields. After addition of 200 μl RIPA buffer to 2 ml of media, cells detached and new images of the same fields were taken to collect reference data on beads' location in nonstressed gel. Images of fluorescent beads were analyzed using image analysis software written in Matlab (courtesy of G. Danuser's and C. Waterman-Storer's groups, The Scripps Research Institute, La Jolla, CA). Images were divided to 1.6-μm^2 areas, and displacement vectors between were calculated (Ji and Danuser, 2005). Vectors (Fig. 5 C, green) on the strain map were increased five times for visualization purposes. Brightfield and strain map images were superimposed using Photoshop (Adobe). Integrated strains were calculated by summing up the magnitudes (WT, 7,400 pixels; and CD98hc null, 1,444 pixels) of the strain vectors inside the cell mask and dividing them by the cell area (WT, 2,945 arbitrary units; and CD98hc null, 1,873 arbitrary units).

Rho GTPase assay

WT and CD98hc-null MEFs were grown in 0.5% serum for 24 h and then in serum-free medium for another 17 h. Cells were detached and kept in suspension at room temperature for 1 h in serum-free medium. Serum-starved cells were then plated on 3D Fn plates (3 million cells/plate), and RhoA activity was assayed at the indicated time points. For LPA treatment, cells were grown and serum starved as described, 1 μg/ml LPA was added to each plate, and RhoA activity was measured after a 5-min incubation. 3D Fn matrix was prepared as described previously (Cukierman et al., 2001) using NIH3T3 cells cultured in a 10-cm Petri dish. RhoA activity was measured using a commercially available ELISA-based assay (G-LISA; Cytoskeleton, Inc.) according to the manufacturer's protocol. Lysates were also resolved by SDS-PAGE and immunoblotted with rabbit anti-RhoA (67B9) antibody (Cell Signaling), followed by a IRDye 800CW goat anti–rabbit IgG (LI-COR Biosciences), and bands were visualized by scanning blots using an infrared imaging system (Odyssey; LI-COR Biosciences).

Online supplemental material

Fig. S1 shows that CD98hc contributes to the integrin-dependent activation of FAK and $p130^{CAS}$ via its integrin binding domain by reconstitution

experiments. The supplemental text provides additional methodological details for the cellular tension measurements and for the assessment of tyrosine phosphorylation. Online supplemental material is available at http://www.jcb.org/cgi/content/full/jcb.200705090/DC1.

Submitted: 15 May 2007
Accepted: 12 July 2007

References

Ali, I.U., V. Mautner, R. Lanza, and R.O. Hynes. 1977. Restoration of normal morphology, adhesion and cytoskeleton in transformed cells by addition of a transformation-sensitive surface protein. *Cell.* 11:115–126.

Arias-Salgado, E.G., S. Lizano, S.J. Shattil, and M.H. Ginsberg. 2005. Specification of the direction of adhesive signaling by the integrin β cytoplasmic domain. *J. Biol. Chem.* 280:29699–29707.

Beningo, K.A., and Y.L. Wang. 2002. Flexible substrata for the detection of cellular traction forces. *Trends Cell Biol.* 12:79–84.

Bissell, M.J., D.C. Radisky, A. Rizki, V.M. Weaver, and O.W. Petersen. 2002. The organizing principle: microenvironmental influences in the normal and malignant breast. *Differentiation.* 70:537–546.

Boucaut, J.C., T. Darribere, S.D. Li, H. Boulekbache, K.M. Yamada, and J.P. Thiery. 1985. Evidence for the role of fibronectin in amphibian gastrulation. *J. Embryol. Exp. Morphol.* 89(Suppl.):211–227.

Boudreau, N.J., and P.L. Jones. 1999. Extracellular matrix and integrin signaling: the shape of things to come. *Biochem. J.* 339:481–488.

Brown, N.H., S.L. Gregory, W.L. Rickoll, L.I. Fessler, M. Prout, R.A. White, and J.W. Fristrom. 2002. Talin is essential for integrin function in *Drosophila*. *Dev. Cell.* 3:569–579.

Checovich, W.J., and D.F. Mosher. 1993. Lysophosphatidic acid enhances fibronectin binding to adherent cells. *Arterioscler. Thromb.* 13:1662–1667.

Chou, F.L., J.M. Hill, J.C. Hsieh, J. Pouyssegur, A. Brunet, A. Glading, F. Uberall, J.W. Ramos, M.H. Werner, and M.H. Ginsberg. 2003. PEA-15 binding to ERK1/2 MAPKs is required for its modulation of integrin activation. *J. Biol. Chem.* 278:52587–52597.

Chrzanowska-Wodnicka, M., and K. Burridge. 1996. Rho-stimulated contractility drives the formation of stress fibers and focal adhesions. *J. Cell Biol.* 133:1403–1415.

Corbett, S.A., and J.E. Schwarzbauer. 1999. Requirements for α(5)β(1) integrin-mediated retraction of fibronectin-fibrin matrices. *J. Biol. Chem.* 274:20943–20948.

Cukierman, E., R. Pankov, D.R. Stevens, and K.M. Yamada. 2001. Taking cell-matrix adhesions to the third dimension. *Science.* 294:1708–1712.

Davidson, L.A., M. Marsden, R. Keller, and D.W. Desimone. 2006. Integrin α5beta1 and fibronectin regulate polarized cell protrusions required for *Xenopus* convergence and extension. *Curr. Biol.* 16:833–844.

Deves, R., and C.A. Boyd. 2000. Surface antigen CD98(4F2): not a single membrane protein, but a family of proteins with multiple functions. *J. Membr. Biol.* 173:165–177.

Diaz, L.A., Jr., A.W. Friedman, X. He, R.D. Kuick, S.M. Hanash, and D.A. Fox. 1997. Monocyte-dependent regulation of T lymphocyte activation through CD98. *Int. Immunol.* 9:1221–1231.

Erickson, H.P. 1994. Reversible unfolding of fibronectin type III and immunoglobulin domains provides the structural basis for stretch and elasticity of titin and fibronectin. *Proc. Natl. Acad. Sci. USA.* 91:10114–10118.

Erickson, H.P. 2002. Stretching fibronectin. *J. Muscle Res. Cell Motil.* 23:575–580.

Fenczik, C.A., R. Zent, M. Dellos, D.A. Calderwood, J. Satriano, C. Kelly, and M.H. Ginsberg. 2001. Distinct domains of CD98hc regulate integrins and amino acid transport. *J. Biol. Chem.* 276:8746–8752.

Féral, C.C., N. Nishiya, C.A. Fenczik, H. Stuhlmann, M. Slepak, and M.H. Ginsberg. 2005. CD98hc (SLC3A2) mediates integrin signaling. *Proc. Natl. Acad. Sci. USA.* 102:355–360.

Francis, S.E., K.L. Goh, K. Hodivala-Dilke, B.L. Bader, M. Stark, D. Davidson, and R.O. Hynes. 2002. Central roles of α5beta1 integrin and fibronectin in vascular development in mouse embryos and embryoid bodies. *Arterioscler. Thromb. Vasc. Biol.* 22:927–933.

George, E.L., E.N. Georges-Labouesse, R.S. Patel-King, H. Rayburn, and R.O. Hynes. 1993. Defects in mesoderm, neural tube and vascular development in mouse embryos lacking fibronectin. *Development.* 119:1079–1091.

George, E.L., H.S. Baldwin, and R.O. Hynes. 1997. Fibronectins are essential for heart and blood vessel morphogenesis but are dispensable for initial specification of precursor cells. *Blood.* 90:3073–3081.

Grinnell, F. 1984. Fibronectin and wound healing. *J. Cell. Biochem.* 26:107–116.

Hall, A. 1998. Rho GTPases and the actin cytoskeleton. *Science.* 279:509–514.

Hughes, P.E., B. Oertli, M. Hansen, F.L. Chou, B.M. Willumsen, and M.H. Ginsberg. 2002. Suppression of integrin activation by activated Ras or Raf does not correlate with bulk activation of ERK MAP kinase. *Mol. Biol. Cell.* 13:2256–2265.

Hynes, R.O. 1994. Genetic analyses of cell-matrix interactions in development. *Curr. Opin. Genet. Dev.* 4:569–574.

Ingber, D. 1991. Integrins as mechanochemical transducers. *Curr. Opin. Cell Biol.* 3:841–848.

Ji, L., and G. Danuser. 2005. Tracking quasi-stationary flow of weak fluorescent signals by adaptive multi-frame correlation. *J. Microsc.* 220:150–167.

Jiang, G., G. Giannone, D.R. Critchley, E. Fukumoto, and M.P. Sheetz. 2003. Two-piconewton slip bond between fibronectin and the cytoskeleton depends on talin. *Nature.* 424:334–337.

Krammer, A., H. Lu, B. Isralewitz, K. Schulten, and V. Vogel. 1999. Forced unfolding of the fibronectin type III module reveals a tensile molecular recognition switch. *Proc. Natl. Acad. Sci. USA.* 96:1351–1356.

Kranenburg, O., M. Poland, M. Gebbink, L. Oomen, and W.H. Moolenaar. 1997. Dissociation of LPA-induced cytoskeletal contraction from stress fiber formation by differential localization of RhoA. *J. Cell Sci.* 110:2417–2427.

Kuo, J.C., W.J. Wang, C.C. Yao, P.R. Wu, and R.H. Chen. 2006. The tumor suppressor DAPK inhibits cell motility by blocking the integrin-mediated polarity pathway. *J. Cell Biol.* 172:619–631.

LaFlamme, S.E., and K.L. Auer. 1996. Integrin signaling. *Semin. Cancer Biol.* 7:111–118.

Lelievre, S.A., V.M. Weaver, J.A. Nickerson, C.A. Larabell, A. Bhaumik, O.W. Petersen, and M.J. Bissell. 1998. Tissue phenotype depends on reciprocal interactions between the extracellular matrix and the structural organization of the nucleus. *Proc. Natl. Acad. Sci. USA.* 95:14711–14716.

Mao, Y., and J.E. Schwarzbauer. 2005. Fibronectin fibrillogenesis, a cell-mediated matrix assembly process. *Matrix Biol.* 24:389–399.

Mautner, V., and R.O. Hynes. 1977. Surface distribution of LETS protein in relation to the cytoskeleton of normal and transformed cells. *J. Cell Biol.* 75:743–768.

McKeown-Longo, P.J., and D.F. Mosher. 1983. Binding of plasma fibronectin to cell layers of human skin fibroblasts. *J. Cell Biol.* 97:466–472.

McKeown-Longo, P.J., and D.F. Mosher. 1985. Interaction of the 70,000-mol-wt amino-terminal fragment of fibronectin with the matrix-assembly receptor of fibroblasts. *J. Cell Biol.* 100:364–374.

Midwood, K.S., L.V. Valenick, H.C. Hsia, and J.E. Schwarzbauer. 2004. Coregulation of fibronectin signaling and matrix contraction by tenascin-C and syndecan-4. *Mol. Biol. Cell.* 15:5670–5677.

Mosher, D.F. 1984. Physiology of fibronectin. *Annu. Rev. Med.* 35:561–575.

Muir, I.F. 1990. On the nature of keloid and hypertrophic scars. *Br. J. Plast. Surg.* 43:61–69.

Ohashi, T., D.P. Kiehart, and H.P. Erickson. 2002. Dual labeling of the fibronectin matrix and actin cytoskeleton with green fluorescent protein variants. *J. Cell Sci.* 115:1221–1229.

Paszek, M.J., N. Zahir, K.R. Johnson, J.N. Lakins, G.I. Rozenberg, A. Gefen, C.A. Reinhart-King, S.S. Margulies, M. Dembo, D. Boettiger, et al. 2005. Tensional homeostasis and the malignant phenotype. *Cancer Cell.* 8:241–254.

Peters, J.H., and R.O. Hynes. 1996. Fibronectin isoform distribution in the mouse. I. The alternatively spliced EIIIB, EIIIA, and V segments show widespread codistribution in the developing mouse embryo. *Cell Adhes. Commun.* 4:103–125.

Ramos, J.W., and D.W. DeSimone. 1996. *Xenopus* embryonic cell adhesion to fibronectin: position-specific activation of RGD/synergy site-dependent migratory behavior at gastrulation. *J. Cell Biol.* 134:227–240.

Ramos, J.W., C.A. Whittaker, and D.W. DeSimone. 1996. Integrin-dependent adhesive activity is spatially controlled by inductive signals at gastrulation. *Development.* 122:2873–2883.

Ren, X.D., W.B. Kiosses, and M.A. Schwartz. 1999. Regulation of the small GTP-binding protein Rho by cell adhesion and the cytoskeleton. *EMBO J.* 18:578–585.

Ruoslahti, E. 1984. Fibronectin in cell adhesion and invasion. *Cancer Metastasis Rev.* 3:43–51.

Schmeichel, K.L., V.M. Weaver, and M.J. Bissell. 1998. Structural cues from the tissue microenvironment are essential determinants of the human mammary epithelial cell phenotype. *J. Mammary Gland Biol. Neoplasia.* 3:201–213.

Schwarzbauer, J.E. 1991. Identification of the fibronectin sequences required for assembly of a fibrillar matrix. *J. Cell Biol.* 113:1463–1473.

Sechler, J.L., Y. Takada, and J.E. Schwarzbauer. 1996. Altered rate of fibronectin matrix assembly by deletion of the first type III repeats. *J. Cell Biol.* 134:573–583.

Sechler, J.L., S.A. Corbett, and J.E. Schwarzbauer. 1997. Modulatory roles for integrin activation and the synergy site of fibronectin during matrix assembly. *Mol. Biol. Cell.* 8:2563–2573.

Sechler, J.L., A.M. Cumiskey, D.M. Gazzola, and J.E. Schwarzbauer. 2000. A novel RGD-independent fibronectin assembly pathway initiated by α4beta1 integrin binding to the alternatively spliced V region. *J. Cell Sci.* 113:1491–1498.

Sechler, J.L., H. Rao, A.M. Cumiskey, I. Vega-Colon, M.S. Smith, T. Murata, and J.E. Schwarzbauer. 2001. A novel fibronectin binding site required for fibronectin fibril growth during matrix assembly. *J. Cell Biol.* 154:1081–1088.

Shattil, S.J. 2005. Integrins and Src: dynamic duo of adhesion signaling. *Trends Cell Biol.* 15:399–403.

Sottile, J., and D.F. Mosher. 1993. Assembly of fibronectin molecules with mutations or deletions of the carboxyl-terminal type I modules. *Biochemistry.* 32:1641–1647.

Tadokoro, S., S.J. Shattil, K. Eto, V. Tai, R.C. Liddington, J.M. de Pereda, M.H. Ginsberg, and D.A. Calderwood. 2003. Talin binding to integrin β tails: a final common step in integrin activation. *Science.* 302:103–106.

Tsumura, H., N. Suzuki, H. Saito, M. Kawano, S. Otake, Y. Kozuka, H. Komada, M. Tsurudome, and Y. Ito. 2003. The targeted disruption of the CD98 gene results in embryonic lethality. *Biochem. Biophys. Res. Commun.* 308:847–851.

van Corven, E.J., A. Groenink, K. Jalink, T. Eichholtz, and W.H. Moolenaar. 1989. Lysophosphatidate-induced cell proliferation: identification and dissection of signaling pathways mediated by G proteins. *Cell.* 59:45–54.

Wang, Y.L., and R.J. Pelham Jr. 1998. Preparation of a flexible, porous polyacrylamide substrate for mechanical studies of cultured cells. *Methods Enzymol.* 298:489–496.

Weaver, V.M., and P. Gilbert. 2004. Watch thy neighbor: cancer is a communal affair. *J. Cell Sci.* 117:1287–1290.

Weaver, V.M., A.H. Fischer, O.W. Peterson, and M.J. Bissell. 1996. The importance of the microenvironment in breast cancer progression: recapitulation of mammary tumorigenesis using a unique human mammary epithelial cell model and a three-dimensional culture assay. *Biochem. Cell Biol.* 74:833–851.

Wierzbicka-Patynowski, I., and J.E. Schwarzbauer. 2002. Regulatory role for SRC and phosphatidylinositol 3-kinase in initiation of fibronectin matrix assembly. *J. Biol. Chem.* 277:19703–19708.

Wierzbicka-Patynowski, I., and J.E. Schwarzbauer. 2003. The ins and outs of fibronectin matrix assembly. *J. Cell Sci.* 116:3269–3276.

Wu, C., A.E. Chung, and J.A. McDonald. 1995a. A novel role for α 3 β 1 integrins in extracellular matrix assembly. *J. Cell Sci.* 108:2511–2523.

Wu, C., A.J. Fields, B.A. Kapteijn, and J.A. McDonald. 1995b. The role of α 4 β 1 integrin in cell motility and fibronectin matrix assembly. *J. Cell Sci.* 108:821–829.

Wu, C., V.M. Keivens, T.E. O'Toole, J.A. McDonald, and M.H. Ginsberg. 1995c. Integrin activation and cytoskeletal interaction are essential for the assembly of a fibronectin matrix. *Cell.* 83:715–724.

Ylanne, J., Y. Chen, T.E. O'Toole, J.C. Loftus, Y. Takada, and M.H. Ginsberg. 1993. Distinct functions of integrin α and β subunit cytoplasmic domains in cell spreading and formation of focal adhesions. *J. Cell Biol.* 122:223–233.

Zhang, Q., W.J. Checovich, D.M. Peters, R.M. Albrecht, and D.F. Mosher. 1994. Modulation of cell surface fibronectin assembly sites by lysophosphatidic acid. *J. Cell Biol.* 127:1447–1459.

Zhong, C., M. Chrzanowska-Wodnicka, J. Brown, A. Shaub, A.M. Belkin, and K. Burridge. 1998. Rho-mediated contractility exposes a cryptic site in fibronectin and induces fibronectin matrix assembly. *J. Cell Biol.* 141:539–551.

Zijlstra, A., N.R. McCabe, and M.E. Schelling. 1999. Expression and assembly of the angiogenic marker B-fibronectin by endothelial cells in vitro: regulation by confluency. *Angiogenesis.* 3:77–87.